

Goaf zone division and index gases of residual coal spontaneous combustion prediction

ZHU Hong-qing, GU Bei-fang, ZHANG Zhen

*Faculty of Resource & Safety Engineering,
China University of Mining & Technology,
Beijing 100083, China*

Abstract

Coal seam spontaneous combustion has become one of the major reasons of coal mine accidents and disasters, which not only seriously threatens the safety mining, but also causes a waste of a great amount of coal resources. To solve the serious problem of residual coal spontaneous combustion in goaf, based on the engineering geological condition of working face, this text simulated stress, strain and plastic distribution of overlying strata in goaf by using FLAC3D numerical simulation software, and based on the nephogram of the stress, strain, plastic zone and change curve of monitoring point, the failure law of overlying strata is analyzed and combined numerical simulation results with empirical formulas, the horizontal and vertical "three zones" range and in goaf were calculated. And studies the law of three typical coal samples between the concentration of CO₂, CO, CH₄, C₂H₄ and coal sample temperature through programmed heating experiment. Based on the simulation and experimental results, determined the distribution range of "three zones" was determined, the index gas CO and auxiliary index gas C₂H₄ were chosen for predicting the coal spontaneous combustion, based on the research, it provided a scientific basis for predicting the residual coal spontaneous combustion and getting the minimum safe speed of advancing working face that will not cause the coal spontaneous combustion in goaf.

Keywords: GOAF; RESIDUAL COAL SPONTANEOUS COMBUSTION; NUMERICAL SIMULATION; "THREE ZONES" DIVISION; TEMPERATURE PROGRAMMED EXPERIMENT; INDEX GAS

1. Introduction

Coal spontaneous combustion seriously affects the mine safety and reduce the mining efficiency. Some coal mines adopt the mining technology of comprehensive mechanization sublevel caving, it lost much coal and the mining rate is low, which seriously cause the residual coal spontaneous combustion in goaf. In order to prevent the coal spontaneous fire in the goaf of fully mechanized caving face, it is necessary to study the goaf "three zones" division after mining the working face and the index gases of coal spontaneous combustion prediction indicator gas in goaf.

The FLAC3D numerical simulation software is based on three-dimensional fast lagrangian analytical procedure, it can simulate the mechanical characteristics of break or plastic flow when geologic materials reach the ultimate

strength or yield limit, especially be suitable for analyzing the instability of the progressive damage and simulating large deformation^[1-3]. Zongxiang Li researched the process of oxygen density consumption and air leakage flow in the isolated coal pillars of the goaf in fully mechanized caving coal face through the numerical simulation method. Rui Wang simulated the failure law of overlying strata during the 8 coal seam was mined in Dong huantuo mine and revealed the distribution law of caving zone, water flowing fractured zone and bend subsidence zone of coal rock seam roof by applying the fluid - solid coupling theory and the FLAC3D numerical simulation software^[5]. Huiyong Yin used FLAC numerical simulation technique to simulate the failure law of overlying strata under the condition of the single coal seam mining conditions the

repeated mining conditions of both upper and the different mining sequence^[6]. Xinyan Si simulated the distribution law of stress, displacement and plastic zone in surrounding rock of the gob-side entries for coal pillar widths of 2, 4, 6, 8, 12, 20 m^[7]. Feng Yang simulated pressure distribution state of tilt direction coal seam^[8]. YongXiu Wang simulated the stress distribution law of the isolated coal pillar in coal mining district, area classification was made according to the stress distribution law of the coal pillar^[9]. The above scholars used numerical simulation technique to simulate some concrete engineering problems by different facets and obtained some results.

Hanpeng Ma used low-temperature oxidation method of temperature programming to research and analysis comprehensively law of index gases coal spontaneous combustion, reveals the main rule of indicator gas during the coal low temperature oxidation process^[10]. Jianhu Ji analyzed the relationship between oxygen absorbed of the spontaneous combustion tendency index and coal quality index of internal factors affecting coal spontaneous combustion, provided a certain theoretical basis to coal spontaneous combustion prevention and control work^[11]. Xiaoxing Zhong analyzed the law of adiabatic oxidation heating rate, oxygen consumption, crossing point temperature during the process of coal spontaneous combustion, pointed out that use single feature parameters of the process of coal spontaneous combustion to incarnate the systemic properties of coal spontaneous combustion, and then came up with the oxidation kinetics method of coal self-ignition orientation^[12]. Bo Tan analyzed change characteristics of each stage of three different metamorphic grade of coal samples^[13]. Zhiqiang Liu probed the indicator gases change rule of the goaf spontaneous combustion, obtained the key parameters of spontaneous combustion prediction, ensured the index and critical value of spontaneous combustion prediction^[14]. Hongqing Zhu ensured the critical temperature of low temperature oxidation index during coal combustion based on adiabatic oxidation test and temperature programmed test, then analysis and calculated spontaneous combustion of low temperature oxidation critical temperature indicator under the different factors by formula of reasoning and linear fitting, researched the relationship between each indicator of correlation analysis and cluster analysis method^[15].

Based on predecessors' research, failure law of goaf overlying strata was simulated by FLAC3D,

three horizontal zones and three vertical zones and permeability were obtained by empirical formulas. The relationship between indicator gas and coal sample temperature of the process of coal spontaneous combustion was researched by coal spontaneous combustion stage characteristic experiment at low temperature, the major indicator gas and auxiliary indicator gas of coal spontaneous combustion prediction were ensured, this text provided reference to coal spontaneous combustion prediction system.

2. Constitutive relation of numerical simulation

The nonlinearity of rock stress-strain curve result from micro-crack produce and extend that is caused by the continuous damage after the rock been stressed and not due to plastic deformation. Therefore, it is suitable to describe the micro-mechanical property of rock by constitutive relation of elastic damage mechanics^[16-17]. For the microscopic structure of the rock. On one hand, because of a large number of joints and fractures, rock is not continuous medium; On the other hand, the rock belongs to crystalline materials, so the rock is not discrete medium, which suggests that rock is a kind of nonlinear material from tectonic nature. The nonlinear nature of rock is presented on the deformation, evolution of rock, the complexity and highly disorder of fracture and pore space distribution and so on.

In the initial state of rock broken, mesoscopic unit is elastic, its mechanical property can completely expressed by the elastic modulus and poisson's ratio. With the unit stress increase, the element began to damage when stress state or strain state of unit meet the given damage threshold. Under the condition of different stress combination, the damage of the rock exhibit two forms: the shear and tensile. Usually, compression failure can be discriminated by the coulomb criterion, tensile failure can be discriminated by maximum tensile-stress criterion. The revised moore cullen criterion can be used as the primitive damage criterion when considering the mesoscopic unit damage under the stress of compress or shear in study area, its characteristic is that tensile failure or shear failure can be considered at the same time, its expression^[18] is

$$\sigma_1 - \frac{1 + \sin \varphi}{1 - \sin \varphi} \geq \sigma_c, (\sigma_3 \geq 0) \quad (1)$$

$$\sigma_3 \leq -\sigma_t, (\sigma_3 < 0) \quad (2)$$

In the formula, σ_1 is maximum principal stress, σ_3 is minor principal stress, Mpa; φ is

internal friction angle, (°); σ_c is axial compressive strength, Mpa; σ_t is uniaxial tensile strength, MPa.

Under the stress state of uniaxial tension, when shear stress reach Mohr-Coulomb damage threshold, the micro constitutive relation of damage is:

$$D = 0, (\varepsilon \geq \varepsilon_{t0}) \quad (3)$$

$$D = 1 - \frac{f_{tr}}{E_0 \varepsilon}, (\varepsilon_{t0} > \varepsilon \geq \varepsilon_{tu}) \quad (4)$$

$$D = 1, (\varepsilon < \varepsilon_{tu}) \quad (5)$$

In the formula, D is damage variable, $D=0$ is no damage state, $D=1$ is completely damage state, $0 < D < 1$ is different level damage degree; f_{tr} is unit residual strength, Mpa; ε_{t0} is tensile strain correspond by elastic limit; E_0 is initial elastic modulus; Mpa.

Under the stress state of uniaxial compression, when shear stress reach the Mohr-Coulomb damage threshold, the micro constitutive relation of damage is:

$$D = 0, (\varepsilon < \varepsilon_{c0}) \quad (6)$$

$$D = 1 - \frac{\lambda \varepsilon_{c0}}{\varepsilon}, (\varepsilon_{c0} \leq \varepsilon) \quad (7)$$

In the fomula, ε_{c0} is the maximum principal strain pressure when maximum principal stress of unit reach uniaxial compressive strength; λ is residual strength coefficient of the unit.

3. Numeric simulation scheme

Based on the practical geological situation of study area, 27 floors coal rock were divided in numerical model, coal thickness is 4m, immediate roof is 6m siltstone, hard roof is 5m fine sandstone, direct bottom is 2m mudstone; coal and rock histogram is shown in figure 1.

Thickness	columnnar 1:200	rock type
		mudstone
6		goaf
3		mudstone coal streak
5		packsand
6		silt-finestone
4		experimental coalseam
2		mudstone
1		coalseam
8		mudstone
4		oolitic mudstone
4		purple mudstone
4		oolitic aluminum mudstone

Figure1. The experimental area working face coal rock of integrated histogram

3.1 Rock mass failure criteria and physical and mechanics parameters

The plastic property of coal that is elastic-plastic material is strong, and it can be regarded as approximate ideal elastic-plastic model, so based on the actual condition, Mohr - Coulomb criterion is chosen as failure criterion, which is $f_t = \sigma_3 - \sigma_t$, $f_s = (\sigma_1 - \sigma_3) - 2c \cos \varphi - (\sigma_1 + \sigma_3) \sin \varphi$, σ_1 is maximum principal stress, σ_3 is minimum principal stress; c , φ , σ_t is respectively cohesion, internal friction angle and tensile strength. When $f_s < 0$, coal will occur shear failure; When $f_t > 0$, coal will occur tensile failure. The gangue fell down from the goaf can be regarded as loose medium, as the working face advancing, the interspace among caving gangue will be compressed gradually and the strength increased gradually, so it can be approximatively represented as the elastic support body. The gangue density ρ , elasticity modulus E and poisson's ratio ν , which all will increased with the time t went, and it can be expressed by the following formula: $\rho = 1600 + 800(1 - e^{-1.25t})$, $E = 15 + 175(1 - e^{-12.5t})$, $\nu = 0.05 + 0.2(1 - e^{-1.25t})$ [19].

The rock mass physical and mechanical parameters for numerical simulation are shown in table 1.

Table1. Coal rock mechanical parameters

Name	Bulk modulus (GPa)	Shear modulus (GPa)	Cohesion (MPa)	Internal friction angle (°)	Tensile Strength (MPa)	Density (kg/m ³)
Coal	1.199	0.368	2	25	0.03	1400
Mudstone	1.613	1.26	3.5	34	0.8	2100
Fine sandstone	2.02	1.709	4.1	33	0.86	2400
Siltstone	5.914	4.622	5	38	1.03	2660

3.2 Numeric Simulation Scheme

The size of model is 300m×300m×150m, it was divided into 393750 units and the strength theory model is Mohr-Coulomb. The set of model boundary conditions are as follows: the around border of model was limited horizontal displacement, x and y horizontal displacement was limited to 0; bottom of the model boundary was fixed, vertical and horizontal direction was limited to 0; top of the model was set as free boundary; the initial vertical stress was apply to the top of the

model, the horizontal vertical stress was apply to the around of the model. First of all, overlying goaf and coal pillar was formed, simulating the advance of excavation face after it reached the balance, simulating the advance of coal seam through null unit. The frequency of excavation is 8m, the time steps is 1000. The width of working face is 200m, the initial excavation position is y= 20m, the end is y=280m, the simulation length is 260m in total. The simplified geometric model is shown in figure 2.

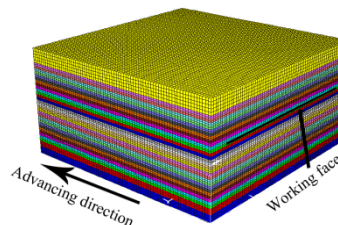
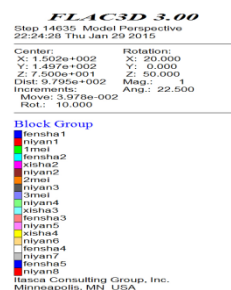


Figure 2. Numerical calculation model

In the process of working face mining, the stress distribution ahead of the working face was shown in figure 3.

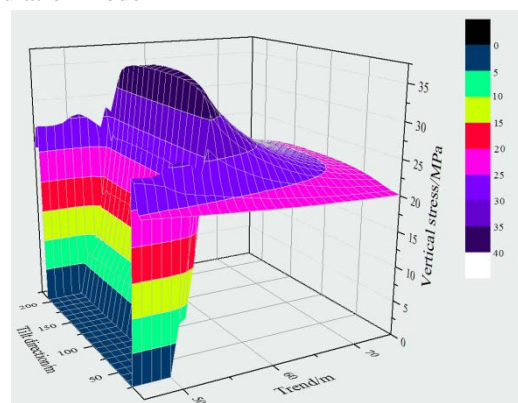


Figure 3. Vertical stress distribution ahead of the working face

Mining production

Figure 3 shows that in front of working face, there exists three zones, relaxation zone, stress concentration zone and original stress zone. After the mining space appeared, the three zones in front of the coal body always exist, and forwards lead as the working face advancing. In the relaxation zone, coal body yield deformation already, a lot of crack are produced in coal body, a lot of coal have broke up already, most part of inner elastic energy released, so the stress in this

zone is low. From relaxation zone to stress concentration zone, stress is increasingly high, so the deformation of coal body largen. In the stress concentration zone, stress to be maximized. Across the peak area and enter the original stress zone, the coal body keeps the original rock stress.

The overlying strata damage of goaf in the process of advancing working face is shown in figure 4.

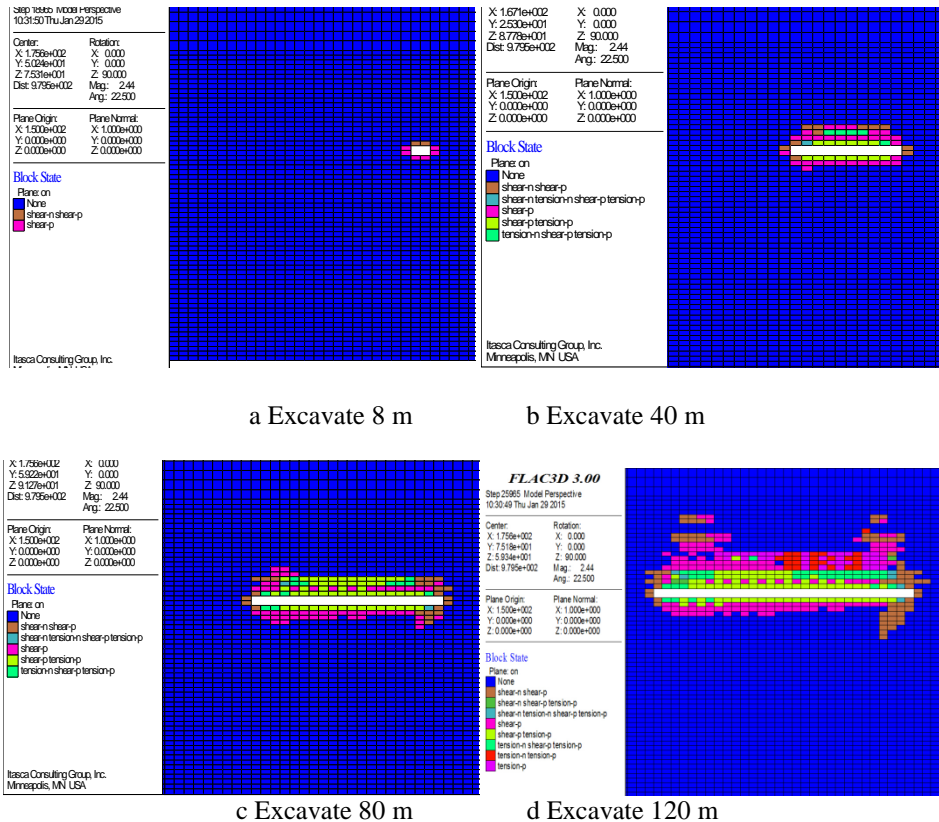


Figure 4. Model unit states of excavation

Figure 4 shows that the fracture began to appear in overlying strata of goaf when the working face excavate to 8 m, the overlying strata fracture development of goaf tend to steady state when the working face excavate to 40m, the main damage types of overlying strata was tensile damage, the overlying strata began to damage in the middle of the excavation section.

Figure 4b shows that the height of fissure zone was about 36m, the main fracture development area was about 0-12 m away from the roof.

4 Overlying strata zones division characteristics of fully mechanized caving face goaf

4.1 The determination of “three zones” in vertical direction

The statistical calculation formulas of caving zone and fractured zone are shown in table 2. The overlying strata of goaf is medium hardness rock, the results that were calculated by the statistical formula are as follows:

$$h_{caving\ zone} = \frac{100 \times 4}{4.7 \times 4 + 19} \pm 2.2 = 10.6 \pm 2.2 \quad (8)$$

$$h_{fissure\ zone} = \frac{100 \times 4}{1.6 \times 4 + 3.6} \pm 5.6 = 40.0 \pm 5.6 \quad (9)$$

Table 2. Caving zone and fissure zone with the height of the statistical formula

Lithology of overlying rock	The height of caving zone/m	The height of fissure zone/m
Hard (40~80Mpa, limestone, quartzite)	$\frac{100m}{2.1m+16} \pm 2.5$	$\frac{100m}{1.2m+2.0} \pm 8.9$
Medium hard (20~40Mpa, argillaceous limestone, arenaceous shale, sandstone, shale)	$\frac{100m}{4.7m+19} \pm 2.2$	$\frac{100m}{1.6m+3.6} \pm 5.6$
Weak (10~20Mpa, mudstone, sandy mudstone)	$\frac{100m}{6.2m+32} \pm 1.5$	$\frac{100m}{3.1m+5.0} \pm 4.0$
Extreme soft (<10Mpa, bauxite, weathered mudstone, clay, sandy clay)	$\frac{100m}{7.0m+63} \pm 1.2$	$\frac{100m}{5.0m+8.0} \pm 3.0$

4.2 The characteristic of horizontal zones

The goaf was divided into natural accumulation zone, load affected zone and compaction stability zone in horizontal direction after roof strata changed and caving rock mass changed in goaf.

Rock caving characteristics of fully mechanized caving face goaf

In the natural accumulation area, hard roof basically kept the original state, some of the gap may exist among caving rock mass and upper roof, the state of caving rock mass was natural accumulation, so the coefficient of bulk increase K_{p1} :

$$K_{p1} = \frac{\sum h - \Delta h + m_1 + m_2 [1 - (1-c)K_{pc}]}{\sum h} \tag{10}$$

In this formula: m_1 —Thickness of mechanical plucking, m; m_2 —The height of caving coal, m; $\sum h$ —The thickness of immediate roof, m; Δh —The gap between roof and falling rock, m; C —Recovery rate of caving coal, %; K_{pc} —Coefficient of bulk increase of goaf residual coal. The fracture rock will produce in the sinking process of rock seam roof in load affected zone, its rotation may has a deformation influence on goaf, the coefficient of bulk increase K_{p2} :

$$K_{p2} = \frac{\sum h + m_1 + m_2}{\sum h} - \frac{L_0(1-C)}{\sum h(L_0-L)} m_2 K_{pc} \tag{11}$$

In this formula: L —Roof control distance of working face, m;

L_0 —Periodic weighting length of working face, m.

In the re-compaction zone, the rock behind the goaf will be compressed again by the sinking roof, the residual hulking coefficient of residual coal in this zone could be replaced by 1, the

coefficient of bulk increase in the re-compaction zone K_{p3} :

$$K_{p3} = \frac{\sum h + m_1 + m_2}{\sum h} - \frac{L_0(1-C)}{\sum h(L_0-L)} m_2 \tag{12}$$

The hulking coefficient of each zone could be calculated after getting the relative parameters, and then the porosity could be calculated.

$$n = 1 - \frac{1}{K_p} \tag{13}$$

In this formula: n —Porosity; K_p —The residual hulking coefficient.

The data in table 3 could be obtained through simulation experiment and field data.

Table 3. Field and simulation experimental data

Parameters	m_1/m	m_2/m	$\Delta h/m$	$\sum h/m$	c	K_{pc}	L_0/m	L/m
Value	3	1	1.1	8	65%	1.1	33	29

Under normal conditions, the structure of voussoir beam and its instability conditions will affect the breaking and caving characteristics of overlying rock mass in goaf, which will result in great change of the hulking coefficient of caving rock mass and coal in goaf. The difference of hulking coefficient will affect air flow pattern in goaf, and affect condition of coal spontaneous combustion in goaf.

4.3 The “three zones” range of horizontal zones in goaf

Based on the simulation experiment results and the moving characteristic of overlying strata, the range of each horizontal zone in goaf are as follows: natural accumulation zone(0~32m), load

Mining production

affected zone(32~90m), compaction stability zone(>90m).

4.4 The division of overlying strata in goaf

Based on the simulation experiment and theoretical formulas, the hulking coefficient of each horizontal zone in goaf can be obtained and the calculation results are as follows: natural accumulation zone is 1.65, load affected zone is 1.71, compaction stability zone is 1.61.

Therefore, the division results of vertical zones and horizontal zones of overlying strata in goaf are shown in table 4 to 5.

Table 4. Division results of vertical zones of overlying rock in goaf

Parameters Name	Range of vertical zones (m)	Porosity
Curve subsidence zone	36~60	-
Fissure zone	12~36	0.2
Caving zone	0~12	0.9

Table 5. Division results of horizontal zones of overlying rock in goaf

Parameters Name	Range of horizontal zones (m)	Porosity
Natural accumulation zone	0~32	0.24
Load affected zone	32~90	0.15
Compaction stability zone	>90	0.13

5 Experimental study of coal spontaneous combustion low-temperature phase feature

5.1 Test system and coal sample preparation

Based on the <Oxidation Kinetics Determination Method of Coal Spontaneous Combustion Tendency >, the experimental system was designed. The system is consist of coal pot system, the programmed temperature-controlling system, the portable gas-distributing system, layout of gas-path and determination of gas-sampling system, experimental control system and data acquisition system. The whole system structure is showed in Figure 5-6.

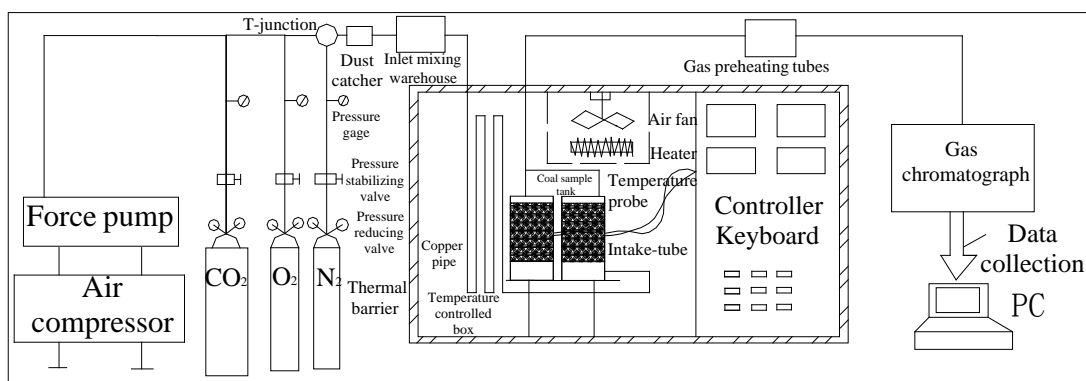


Figure 5. Schematic diagram of experimental system



Figure 6. Entity diagram of experimental system

The experimental coal samples are taken from residual coal pillar, pillar intake airflow roadway, pillar return airway. The gas of seal bag was extracted and was analyzed by chromatography, which was taken as the coal sample gas at room temperature.

Opened the seal bag and crushed the coal samples, the crushed coal samples were sieved by using five different mesh sieves, obtaining the five kind particle sizes coal samples each 150g, which the particle sizes include <0.9mm, 0.9~3mm, 3~5mm, 5~7mm, 7~10mm, mixing all the experimental coal samples that is total 750g and loading in coal pot immediately. Temperature of

the experimental apparatus should be controlled between 20 degrees and 200 degrees, air inlet flow is 100ml/min.

5.2 Experimental results

Experimental aim is to determinate the gas outlet composition and concentration at different temperature in the process of coal low-temperature oxidation, and to study the law between the coal temperature and the gas outlet concentration and determine the index gases. The gas concentration of three coal samples are shown from table 6 to table 8 at the outlet side of coal pot in the process of coal low-temperature oxidation.

Table 6. Gas concentration of coal sample 1 in the process of coal temperature oxidation

t(°C)	Gas concentration of outlet				
	C _{O2} (%)	C _{CO} (PPM)	C _{CO2} (PPM)	C _{CH4} (PPM)	C _{C2H2} (PPM)
25	20.857	9.987	1099.084	184.245	0.181
40	20.682	12.768	1571.531	485.698	0.349
70	20.388	54.548	3502.832	2026.867	0.179
100	19.723	343.387	9209.098	3951.848	0.965
130	19.287	531.778	8956.691	4101.036	2.089
160	17.398	2486.491	12614.318	4299.697	5.433
190	15.207	5599.340	30829.231	4458.827	15.045
205	14.065	7301.057	33127.258	4602.603	29.942

Table 7. Gas concentration of coal sample 2 in the process of coal temperature oxidation

t(°C)	Gas concentration of outlet				
	C _{O2} (%)	C _{CO} (PPM)	C _{CO2} (PPM)	C _{CH4} (PPM)	C _{C2H2} (PPM)
25	20.537	23.288	1571.788	494.060	0.030
40	20.367	29.391	2532.520	817.925	0.087
70	20.050	82.155	6786.801	3072.110	0.246
100	19.864	280.798	11443.112	3876.965	0.602

130	19.335	626.843	16582.670	3991.957	1.195
160	17.419	2314.960	20336.166	4534.242	5.814
190	15.043	5484.399	31575.674	4690.490	17.589
205	14.093	8736.722	38788.012	4484.010	27.350

Table 8 Gas concentration of coal sample 3 in the process of coal temperature oxidation

t(°C)	Gas concentration of outlet				
	C _{O2} (%)	C _{CO} (PPM)	C _{CO2} (PPM)	C _{CH4} (PPM)	C _{C2H2} (PPM)
25	20.864	15.040	2861.607	2428.261	0.179
40	20.738	18.001	3551.389	2793.423	0.367
70	20.299	61.282	8354.916	4013.284	0.254
100	20.196	236.411	10241.866	3987.065	1.004
130	19.853	341.076	7250.034	3630.745	1.586
160	17.783	1605.430	12968.450	4151.353	5.392
190	16.250	4491.810	25199.258	4333.921	14.237
205	15.911	5918.685	25471.063	4220.018	22.308

5.3 Index gas analysis and determination

Different experimental coal samples will result in the difference in the gases produced by the reaction between coal and oxidation, and its composition, concentration, curve of varying with temperature in the process of coal low-temperature oxidation. Index gases are characteristic among the materials produced by fire, and its can reflect the corresponding temperature of the different generation amount, and are able to forecast the fire, which have great practical significance for the early warning of abandoned-coal spontaneous combustion disaster in underground goaf.

5.3.1 Changes relationship between CO₂ and coal temperature

The experimental results of CO₂ are shown in Figure 7, the conclusions that can be drawn from the Figure 7 are as follows:

(1) CO₂ has been existed during the first measurement, and the main reason is that a certain amount of CO₂ exists in the air, and it is difficult to determine the initial resolution time of CO₂.

(2) Generation rate of CO₂ increased significantly after 55 degrees; generation amount of CO₂ showed a rapid decline between 100 degrees and 130 degrees, which was caused by water gasification at about 100 degrees in coal, and this illustrates that water vaporization has an obvious impact in the generation amount of CO₂.

(3) Generation amount of CO₂ showed a rapid increase after 130 degrees. Good regularity does not exist between the CO₂ generation amount of three coal samples and the temperature.

(4) The external environment has a tremendous impact in the determination results of CO₂, which result in obvious regularity does not exist between the generation amount of CO₂ and the temperature. Different coal samples amounts also have a great impact on the generation amount of CO₂ by comparing to three coal samples diagram of the generation amount of CO₂ and the temperature, there is a big difference between the CO₂ generation amount of each coal sample and the temperature, and the unified trends cannot be obtained.

In summary, good regularity does not exist between CO₂ and temperature, and it cannot be used as the index gas of predicting coal spontaneous combustion.

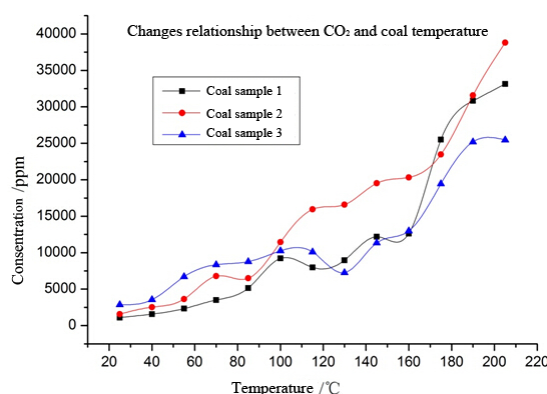


Figure 7. Change curve of CO₂ concentration with temperature

5.3.2 Changes relationship between CO and coal temperature

Significant exponential relationship exists among the CO generation amount and temperature in the early coal oxidation during the coal low-temperature oxidation. And its regularity is strong, the generation amount is large, which is shown in Figure 8, the conclusions can be obtained from Figure 8 are as follows:

(1) CO of three coal samples has been generated at about 30 degrees; there is an exponential relationship between generation amount and temperature, as the temperature increases, CO production rate increases and the growth is rapid at about 130 degrees, it presents a strong regularity, and exhibits a good exponential relationship with temperature.

(2) It keeps growing between the CO generation amount and temperature from 70 degrees to 100 degrees, CO generation amount is almost zero, which is caused by water gasification at about 100 degrees in coal; compared with the correlation between CO₂ and temperature, the effect that water vaporization affects CO is significantly smaller; the CO generation amount increase sharply when it is over 130 degrees.

(3) Some error should be specially noted between the actual measured value and the experimental obtained value when applying the index gas CO to the field, and the main reason is that coal spontaneous combustion generally occurs in mined-out area or coal column during the daily production of coal mine, the air leakage condition in goaf and hypoxia affect the CO practical generation amount seriously, in order to forecast accurately, the CO index gas should be combined with the derivative index that include the CO index and fire coefficient, and so on.

In summary, CO can be used to forecast the early coal spontaneous combustion, and it is a highly sensitive indicator so that it can be used as the iconic gas of forecasting coal spontaneous combustion.

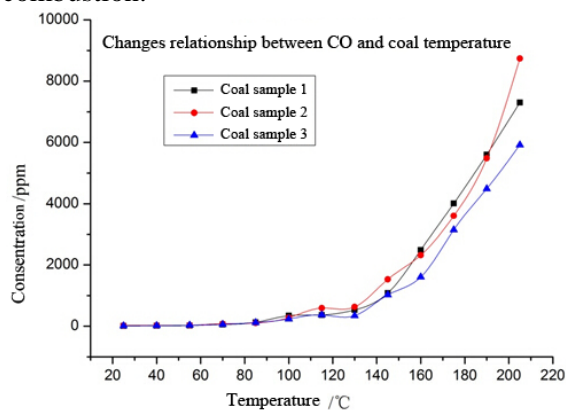


Figure 8. Change curve of CO concentration with temperature

5.3.3 Changes relationship between CH₄ and coal temperature

The experimental results of CH₄ are shown in Figure 9, the conclusions that can be obtained from Figure 9 are as follows:

(1) CH₄ of three coal samples has been generated at near room temperature and the increasing trend is obvious, which mainly depends on the characteristics of the coal sample itself; the generation rate suddenly drops from 115 degrees to 130 degrees, which is caused by the desorption of the adsorptive CH₄ in coal before 115 degrees and CH₄ generation amount trend is flat after 130 degrees.

(2) The CH₄ generation amount of three coal samples basically appear logarithmic growth during experimental temperature range.

In summary, combined with analysis of three coal samples, CO show a certain regularity and can be used as the iconic gas of forecasting coal spontaneous combustion.

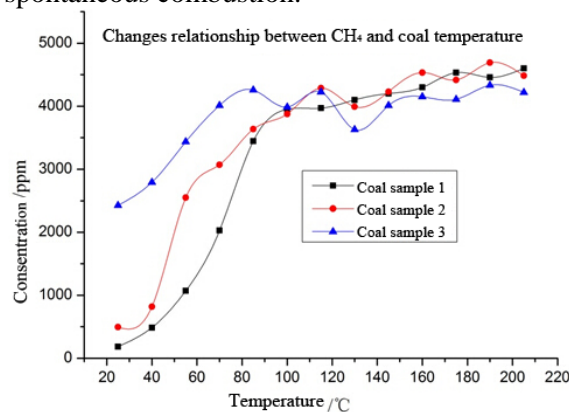


Figure 9. Change curve of CH₄ concentration with temperature

5.3.4 Changes relationship between C₂H₄ and coal temperature

The experimental results of C₂H₄ are shown in Figure 10, the conclusions that can be drawn from Figure 10 are as follows:

(1) C₂H₄ of three coal samples has been generated after 100 degrees and showed a rapid growth rate after 130 degrees.

(2) The corresponding relation keeps unanimous between the C₂H₄ generation amount of each coal sample and the temperature, and they showed an exponential relationship and have a good regularity.

(3) Water gasification has an important impact on the C₂H₄ generation amount from 100 degrees to 130 degrees.

Because of the olefin gas does not exist in the adsorptive gas in coal, and different coal samples will generate a large amount of C₂H₄ at about 160 degrees, coal sample temperature has

reached or exceeded 160 degrees if the C_2H_4 can be determined in the coal mine, which means that it has reached the accelerated oxidation stage of coal spontaneous combustion. However, the generation amount of C_2H_4 is very little at below 100 degrees so that it only can be detected by high precision measuring instruments, so it can be used as the auxiliary iconic gas of forecasting coal spontaneous combustion.

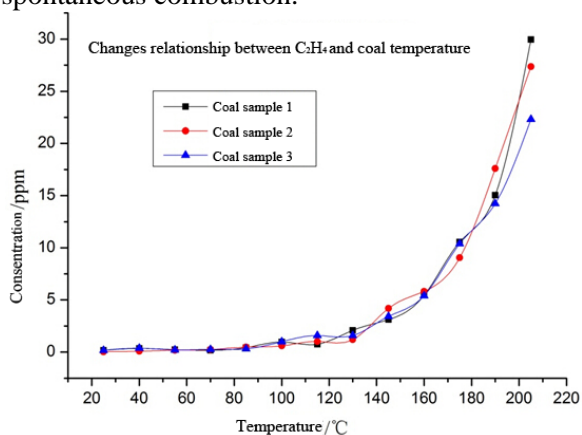


Figure 10. Change curve of C_2H_4 concentration with temperature

Conclusion

(1) With the working face advancing, the caving zone height of overlying strata in goaf increased; and it will no obvious changes after three periodic pressures, which will maintain at about 20m and the development of bed separation fissure was faster than that of fracture fissure. Usually, the covered rock separation strata will change after the working face advanced about 6~9m, and its scope and location will expand and increase, which will intensify after the overlying strata fractured.

(2) In the vertical direction, the overlying strata is divided into caving zone, fissure zone and bending zone in the order that is from bottom to top, their scope respectively is 0~12m, 12~36m and >60m; In the horizontal direction, the goaf is divided into natural accumulation zone, load affected zone and compaction stability zone and their scope respectively is 0~32m, 32~90m and >90m.

(3) It showed an obvious exponential relation between CO generation amount and temperature, and its generation amount is large, which presented a strong regularity; The obvious regularity cannot found between CO_2 generation and temperature; the CH_4 generation amount showed an logarithmic growth, which overall exhibit certain regularity; the relation is basically unanimous between C_2H_4 generation and

temperature, and showed an exponential form, which has good regularity.

(4) Combined with experiment analysis, the CO can be used as the iconic gas of forecasting coal spontaneous combustion, while the C_2H_4 was used as the auxiliary iconic gas.

References

1. Wu Ai-xiang, Huang Ming-qing, Han Bin et al. Orthogonal design and numerical simulation of room and pillar configurations in fractured stopes[J]. Journal of Central South University, 2014,21(8):3338-3344.
2. SUN Shu-wei, LIN Hang, REN Lian-wei. FLAC3D application in geotechnical engineering[M]. Beijing: China Water Power Press, 2011.
3. CHEN Yu-min. FLAC\FLAC3D infrastructure and project examples[M]. Beijing: China Water Power Press, 2009.
4. [4] LI Zong-xiang, SUN Guang-yi, WANG Ji-bo. Numerical simulation of leakage and oxygen consumption in coal pillar of comprehensive coal face[J]. Mechanics in Engineering, 2001,(04):15-18.
5. WANG Rui, MENG Shao-ping, XIE Xiao-tong, etc. Waterproof coal pillar reasonable design and numerical simulation under extremely thick unconsolidated strata[J]. Coal Geology & Exploration, 2011,(01):31-35.
6. YIN Hui-yong, WEI Jiu-chuan, WANG Huai-wen, etc. Study on establishment of artificial mine boundary coal pillar based on numerical simulation[J]. Mining Safety & Environmental Protection, 2013,(02):12-15.
7. SI Xin-yan, WANG Wen-qin, SHAO Wen-gang. Numerical research on reasonable width of coal pillar in the double gob-side entries[J]. Journal of Mining & Safety Engineering, 2012,(02):215-219.
8. YANG Feng, WANG Lian-guo, XU Dong-lai. Numerical simulation study on coal pillar size optimization of roadway driving along gob[J]. China Mining Magazine, 2008,(04):70-72.
9. WANG Yong-xiu, QI Qing-xin, CHEN Bing, etc. Analysis on digital simulation for stress distribution law of coal pillar[J]. Coal Science and Technology, 2004,(10): 59-62.
10. MA Han-peng, LU Wei, WANG Bao-de. System study on the index gases

- generation regular of coal spontaneous combustion process [J]. *Mining Safety & Environmental Protection*, 2007,(06):4-6.
11. JI Jian-hu, XIE Qiang-yan, WANG Chang-yuan. Analysis on the factors of coal spontaneous combustion[J]. *Mining Safety & Environmental Protection*, 2008,(03): 24-26.
 12. ZHONG Xiao-xing, WANG Deming, QI Xuyao, etc. Research on oxidation kinetics test methods concerning the spontaneous combustion of coal[J]. *Journal of China University of Mining & Technology*, 2009,(06):789-793.
 13. TAN Bo, HU Rui-li, GAO Peng, etc. Temperature-programmed experimental study on stage characteristics of coal spontaneous combustion disaster gas indicators[J]. *China Safety Science Journal*, 2013,(02):51-57.
 14. LIU Zhi-qiang. Research on prediction index and alert value of spontaneous combustion in gob[J]. *Coal mining Technology*, 2013,(02): 99-102.
 15. ZHU Hong-qing, WANG Hai-yan, HU Rui-li, etc. Analysis on correlativity between indexes of coal spontaneous combustion critical temperature with low temperature oxidation[J]. *Coal Science and Technology*, 2013,(08):61-64.
 16. YANG Tian-hong, TANG Chun-an, XU Tao, etc. Seepage characteristic in rock failure-theory,model and application[M]. Beijing: Science press, 2004.
 17. CHENG Yuan-ping, YU Qi-xiang. Experimental research of safe and high-efficient exploitation of coal and pressure relief gas in long distance[J]. *Journal of China University of Mining & Technology*, 2004,33(2):132-136.
 18. LIU Hong-yuan, LIU Jian-xin, TANG Chun-an. Numerical simulation of failure process of overburden rock strata caused by mining excavation[J]. *Chinese Journal of Geotechnical Engineering*, 2001,23(2):201-204.
 19. Xie He-ping, Zhou Hong-wei, Wang Jin-an, etc. Application of FLAC to predict ground surface displacements due to coal extraction and its comparative analysis[J]. *Chinese Journal of Rock Mechanics and Engineering*, 1999, 18(4): 397-401.